On the phase diagram of a two-dimensional electron–hole system

Oleg L. Berman, Roman Ya. Kezerashvili, Klaus G. Ziegler

Angaben zur Veröffentlichung / Publication details:

Berman, Oleg L., Roman Ya. Kezerashvili, and Klaus G. Ziegler. 2015. "On the phase diagram of a two-dimensional electron–hole system." *Physica E: Low-dimensional Systems and Nanostructures* 71: 7–13. https://doi.org/10.1016/j.physe.2015.03.016.

On the phase diagram of a two-dimensional electron–hole system

Oleg L. Berman [a,b,*], Roman Ya. Kezerashvili [a,b], Klaus Ziegler [c]

[a] *Physics Department, New York City College of Technology, The City University of New York, Brooklyn, NY 11201, USA*
[b] *The Graduate School and University Center, The City University of New York, New York, NY 10016, USA*
[c] *Institut für Physik, Universität Augsburg, D-86135 Augsburg, Germany*

1. Introduction

An electron–hole system, where the electrons reside in a two-dimensional layer and the holes in another two-dimensional layer (see Fig. 1), represents a many-body system with controllable attractive Coulomb interaction and controllable density. For weak attraction the Bardeen–Cooper–Schrieffer (BCS) approach predicts the formation of coherent Cooper pairs, whereas strong attraction results in the formation of composite bosons, known as indirect (dipolar) excitons. The crossover between the two regimes is not easy to identify because both consist of coherent bosonic states. Besides these two fundamental regimes other phases may exist, because the physics goes beyond the weakly interacting electron gas in conventional superconductors, where the attraction is created by electron–phonon coupling [1,2]. In particular, at higher densities and sufficiently high temperatures new phases could appear when the rate of fermionic collisions increases which leads to an electron–hole plasma (EHP). On the other hand, we can increase the density at a fixed temperature by increasing the Fermi energy. Since the Cooper pairs have a repulsive interaction due to Pauli's principle, even if the repulsive Coulomb interaction is screened, there is an upper limit for their density. The limit can be understood in the following fermionic picture: the electrons and hole in a realistic system have finite bands with an upper band edge E_b. (For simplicity we assume that E_b is the same for electrons and holes.) As long as the Fermi energy is less than the upper band edge, a sufficient Coulomb attraction creates coherent Cooper pairs with a gapless spectrum. The excitation of individual fermions is suppressed by the BCS gap, though. If the Fermi energy exceeds the upper band edge there are still electron–hole pairs but with a gapped spectrum because both, electron and hole, must be excited above the Fermi surface, as depicted in Fig. 2. Now it depends on how strong the Coulomb interaction is in comparison with the thermal fluctuations. If the first is stronger than the latter, we excite electron–hole pairs. Such a state has some similarity

* Corresponding author at: Physics Department, New York City College of Technology, The City University of New York, Brooklyn, NY 11201, USA.
E-mail address: oberman@citytech.cuny.edu (O.L. Berman).

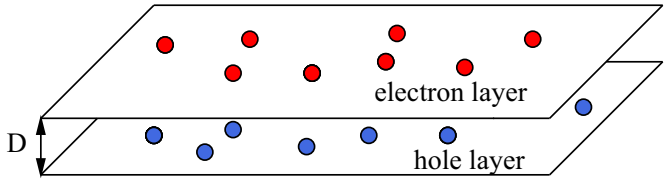

Fig. 1. The formation of an electron–hole gas in two parallel layers separated by distance D, where the electrons reside in one, the holes in the other layer.

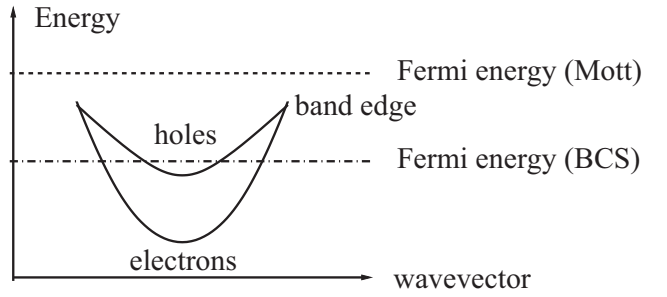

Fig. 2. The schematic electron–hole dispersion with an upper band edge indicates two qualitatively different situations: pairs with gapped spectrum are formed when the Fermi energy is above the band edge.

with a bosonic Mott state [3,4]. In the opposite case we would excite electrons or hole individually which leads to an EHP [5,6].

Here it should be noticed that a quantum phase transition of a Bose gas on a lattice from a Bose Einstein condensate or a superfluid to a Mott insulator phase was discussed by Fisher et al. some time ago [3]. In this work the transition was treated in mean-field approximation, which was later used by many other researchers (see Ref. [4] and references therein). The predicted quantum phase transition was later observed experimentally by Greiner et al. in an ultracold gas of ^{87}Rb atoms in an optical lattice [7]. From the theoretical point of view, the situation is similar in a gas of Cooper pairs that consist of electrons and holes, when we consider a system with a finite momentum cutoff. The latter implies a finite cut-off for the wavevector that plays the role of the lattice constant in the optical lattice of the ultracold gases.

The double layer system depicted in Fig. 1 can be realized in the form of coupled quantum wells (CQWs) or by two graphene layers (GLs). The CQWs are conceptually simple: negative electrons are trapped in a two-dimensional plane, while an equal number of positive holes are trapped in a parallel plane at a distance D. Various electron–hole phases, characterized by unique collective behavior, have been studied in the system of spatially separated electrons and holes. Superfluidity in CQWs has been predicted in terms of the BCS mean-field approach [8], which stimulated intensive theoretical [9–17] and experimental studies [18–26]. Other theoretical studies considered the BCS phase of electron–hole Cooper pairs in a dense electron–hole system [8] and a dilute gas of dipolar excitons, where the latter are formed as bound states of electron–hole pairs in CQWs [27]. Besides the superfluid phase a Wigner supersolid state due to dipolar repulsion was proposed in electron–hole bilayers [28].

There were also performed various experiments devoted to the studies of the collective properties of the phases in an electron–hole bilayer. The recent progress in the theoretical and experimental developments in the studies of the condensate dipolar exciton in coupled quantum wells was reviewed in Ref. [29]. The experimental progress towards probing the ground state of an electron–hole bilayer by low temperature transport was reviewed in Ref. [30], and the summary of experimental studies of excitonic phases in CQWs is presented in Ref. [31].

Besides the condensation of excitons and the formation of a superfluid state, their dissociation into the electron–hole plasma was studied experimentally for GaAs/AlGaAs CQWs in Ref. [32]. The phase diagram of indirect excitons formed by the spatially separated electrons and holes in GaAs/AlGaAs CQWs was analyzed experimentally, and it was shown that the exciton system undergoes a phase transition to an unbound electron–hole plasma for increasing temperatures [32]. This transition has been manifested as an abrupt change in the photoluminescence linewidth and in the peak energy at some critical power density and temperature. The dynamics of the ionization transition of the excitons was studied by using the rate equation [33]. The fraction of ionized carriers in an electron–hole-exciton gas in a photoexcited semiconductor was derived theoretically by applying the mass-action equation, or Saha equation, for the number of free carriers in equilibrium [34].

Within the Hartree–Fock approximation the ionization equilibrium of an electron–hole plasma and the exciton phase was investigated in a highly excited semiconductor in Ref. [35] with special attention to the influence of many-particle effects such as screening and lowering of the ionization energy. The dissociation of excitons in GaAs-GaAlAs quantum wells with increasing excitation was studied [36].

The condensation of Cooper pairs formed by spatially separated electrons and holes was also the subject of more recent studies in a system of two isolated graphene layers [37,38]. The electron-electron interactions in decoupled GLs were analyzed in detail, where it was found that the Hartree–Fock approach provides a quite accurate description of the inter-particle interactions in GLs [39]. The electron–hole superfluidity caused by formation of the BCS phase by Cooper electron–hole pairs in two parallel bilayer graphene sheets was proposed recently [40], where also the Hartree–Fock approximation was applied. In Ref. [41] the superfluidity of quasi-two-dimensional dipole excitons in double-layer graphene was predicted in the presence of band gaps.

According to a detailed study of the ionization degree of the electron–hole plasma in semiconductor quantum wells [42], the dependence of the degree of ionization on the carrier density depends dramatically on the electron and hole masses and the dielectric constant, which are different for different semiconductors. In Ref. [42] the phase transition between the exciton phase and the EHP was analyzed. It should be emphasized that the transition from an exciton gas to an EHP could have important applications to all-optical switching [43–45].

In this paper we study the phase diagram of double layer system in Fig. 1. Within a BCS-like approach we will be able to distinguish three different phases: a BCS phase, an EHP and a bosonic Mott phase.

The paper is organized in the following way. In Section 2 the model Hamiltonian of two-layer electron–hole system is introduced. The mean-field approximation, applied to the system under consideration, is described in Section 3. The phase diagram of a translational invariant electron–hole system is presented in Section 4. Finally, the discussion of the results and conclusions follow in Sections 5 and 6, respectively.

2. Model hamiltonian

The Hamiltonian of a spinless electron–hole system in momentum representation can be written as

$$H = \sum_{\mathbf{k}} \sum_{\sigma=e,h} (\epsilon_{\mathbf{k},\sigma} - \mu_\sigma) c^\dagger_{\mathbf{k}\sigma} c_{\mathbf{k}\sigma} + \sum_{\mathbf{k},\mathbf{q},\mathbf{q}'} U_{\mathbf{k}} c^\dagger_{\mathbf{k}-\mathbf{q},h} c_{\mathbf{k}-\mathbf{q}',h} c^\dagger_{\mathbf{q},e} c_{\mathbf{q}',e}, \quad (1)$$

where $c^\dagger_{k,e}$ ($c_{k,e}$) is the creation (annihilation) operator for electrons, and $c^\dagger_{k,h}$ ($c_{k,h}$) is the corresponding operator for holes, μ_σ is the

chemical potential of fermions, assuming that they are adjusted in such a way that the densities of electrons and holes are equal in order to have a neutral electron–hole plasma, which is justified by the fact that the electrons and holes are created always pairwise by an external laser source. The spin of electrons and holes is neglected here because we are not interested in magnetization effects. Moreover, we assume the simple parabolic dispersion relations $\epsilon_{\mathbf{k},e} = k^2/2m_e$, $\epsilon_{\mathbf{k},h} = k^2/2m_h$ for the electrons and holes with effective electron m_e and hole m_h masses, respectively. To take care of the band structure of a realistic system we introduce an upper cut-off energy E_b in such way that the kinetic energy of the quasiparticles is constrained by $0 \le \epsilon_{\mathbf{k},e} + \epsilon_{\mathbf{k},h} \le E_b$. In Eq. (1) $U_{\mathbf{k}}$ is the attractive electron–hole interaction, that is different for the paired electrons and holes in CQWs and two separated graphene layers and can be defined by the 2D Fourier image of the screened electron–hole attraction $U(\mathbf{r})$ as [8]

$$U_{\mathbf{k}} = -\frac{\hbar\bar{U}\ \exp(-kD/\hbar)}{k + 2\hbar(a_e^{-1} + a_h^{-1}) + 4\hbar^2(1 - \exp(-2kD/\hbar))/(a_e\, a_h\, k)}. \quad (2)$$

In Eq. (2) $a_{e,h} = \hbar^2\varepsilon/(\kappa e^2 m_{e,h})$, D is the thickness of the dielectric interlayer, $\bar{U} = 2\pi\kappa e^2/(\varepsilon l_F^2)$ is the interaction strength, where $\kappa = 9\times 10^9\ \mathrm{Nm^2/C^2}$, e is the electron charge, ε is the dielectric constant of the CQWs or the dielectric between GLs, $l_F = 2\sqrt{\pi/n}$ is the Fermi wavelength with n that is the density of electrons and holes. It is clear that $U_{\mathbf{k}}$ is different for the paired electrons and holes in CQWs and two separated GLs because the effective masses for electrons and holes in these system are different. The interaction strength $U_{\mathbf{k}}$ can be controlled by changing the interlayer separation D and placing dielectrics with different dielectric constant ε.

The Fermi momentum and the Fermi energy of the 2D Fermi system are defined as $q_F = \hbar\sqrt{\pi n}$, and $E_{F(e,h)} = q_F^2/2m_{e,h}$, respectively. Estimating $q_F D$ for the parameters of the real quantum wells, we obtain $q_F D/\hbar \ll 1$, and we use the following approximation for the potential energy of the electron–hole attraction given by Eq. (2):

$$U_{\mathbf{k}} \approx -\frac{\hbar\bar{U}e^{-kD/\hbar}}{k + a}, \quad (3)$$

where a is a material dependent parameter given by

$$a = 2\hbar(a_e^{-1} + a_h^{-1} + 4Da_e^{-1}a_h^{-1}). \quad (4)$$

Now we consider the grand-canonical equilibrium of the electron–hole gas, and define the expectation value of the operator O with respect to the Boltzmann distribution $\exp(-\beta H)$ at temperature T and the trace with respect to all fermionic quantum states of the Hamiltonian H as

$$\langle O\rangle = \frac{1}{Z}\ \mathrm{Tr}[e^{-\beta H}O], \quad Z = \mathrm{Tr}[e^{-\beta H}], \quad (5)$$

where $\beta = 1/k_B T$. The free energy F then reads $F = -k_B T\ \log Z$, from which we obtain the densities of electrons and holes as

$$\langle n_{e,h}\rangle = -\frac{\partial F}{\partial \mu_{e,h}}, \quad (6)$$

where μ_e and μ_h are the chemical potentials of the electron and hole systems, respectively.

3. Free energy of the system

To study the phase diagram for the phase transitions in the system of spatially separated electrons and holes in coupled quantum wells or graphene double layers one should find the free energy of the system and choose some method to compute the free energy. The next step is to find the minima of the free energy as a function of the adjustable parameters. By determining phase that has the lower free energy at each point in parameter space one can construct the phase diagram. There are different approaches to approximately compute the free energy. In order to evaluate the free energy of the interacting electron–hole system we apply a mean-field approximation. A mean-field approximation was applied successfully to study Mott transition superfluid-insulator as described in Refs. [3,4]. The ground state of the 2D electron–hole system was analyzed in the framework of a mean-field approximation, for example, in Refs. [8,15,16,35]. The superfluid-Mott insulator transition was analyzed in the mean-field framework by the expansion of the action in powers of the order parameter [3]. We follow a similar procedure for the expansion of the free energy in powers of the order parameter at finite temperatures and apply a mean-field approximation to obtain not only ground state energy, but also the free energy of the system at nonzero temperatures. In our approach the advantage to use the mean-field approximation is that one can obtain the analytical results for the free energy and conduct the simple analysis of phase diagram.

Our mean-field approach is based on the idea that we replace the interaction terms in the Hamiltonian (1), which are quartic expression with respect to the fermion operators, by a quadratic term that couples to a mean field. There are several options for choosing the mean field. Very common is to use a Hartree–Fock like approximation that couples to the fermion densities $c^\dagger_{\mathbf{k},\sigma}c_{\mathbf{k},\sigma}$ [35]. Then the mean field is a self-energy $i\Sigma''_{\mathbf{k},\sigma} + \Sigma'_{\mathbf{k},\sigma}$, where the real part $\Sigma'_{\mathbf{k},\sigma}$ describes a shift of the Fermi energy and the imaginary part $\Sigma''_{\mathbf{k},\sigma}$ a damping of the quantum dynamics. An alternative choice is to consider a complex mean field $\Delta_{\mathbf{k}}$ that corresponds to BCS pairing [8]:

$$\sum_{\mathbf{k},\mathbf{q},\mathbf{q}'} U_{\mathbf{k}} c^\dagger_{\mathbf{k}-\mathbf{q},h} c_{\mathbf{k}-\mathbf{q}',h} c^\dagger_{\mathbf{q},e} c_{\mathbf{q}',e} \approx \sum_{\mathbf{k}} \Delta_{\mathbf{k}} c_{\mathbf{k},e} c_{-\mathbf{k},h} + h.\,c.\,, \quad (7)$$

where the mean field $\Delta_{\mathbf{k}}$ is the usual order parameter of the BCS theory. In the latter case we can assume that the effective shift of the Fermi energy by the self-energy is already taken into account, which implies that the Fermi energy is the renormalized one. Within this approximation we can perform the trace in Eq. (5) with respect to non-interacting electrons and holes. These states are created as product states by applying the fermionic creation and annihilation operators $c^\dagger_{\mathbf{k},e}$ ($c_{\mathbf{k},e}$) and $c^\dagger_{\mathbf{k},h}$ ($c_{\mathbf{k},h}$) of Eq. (1) to a vacuum state. Then the free energy in momentum representation reads (cf. Ref. [46])

$$F = -\frac{1}{(2\pi q_F)^2}\left[\int_{q\le q_F} \frac{\Delta_{\mathbf{q}}\Delta_{-\mathbf{q}}}{U_{\mathbf{q}}}\, d^2q + \beta\int_{q^2/2m_+\le E_b} \ln(1 + e^{-2\beta E_q} + 2e^{-\beta E_q}\ \cosh[\beta\sqrt{RE_q^2 + |\Delta_{\mathbf{q}}|^2}])\, d^2q\right], \quad (8)$$

where $E_q = (q^2 - q_F^2)/2m_-$ is the single particle energy with $m_\pm = m_e m_h/(m_h \pm m_e)$ and $R = m_-^2/m_+^2 = (m_h + m_e)^2/(m_h - m_e)^2$. It should be noticed that we consider the case where the masses of the electrons and holes are different. This results in the extra term related to R in Eq. (8). When the effective masses of the electrons and holes are equal this term vanishes. Now the gap order parameter $\Delta_{\mathbf{q}}$ is determined as the minimum of the free energy. The density of particles can be evaluated using Eq. (6), which allows us to fix the Fermi energy $E_{F(e,h)}$ by adjusting the average density $\langle n\rangle$ with the experimental results. This allow us to calculate first the pairing order parameter $\Delta_{\mathbf{q}}$ as the minimum of the free energy, after inserting the solution in F, then the average

density $\langle n \rangle$.

By increasing the laser pumping intensity, the electron–hole density increases and one can observe a phase transition from a dilute electron–hole plasma to a BCS phase of paired electron–hole system and another phase transition from the BCS phase to a dense EHP. Both phase transitions are the second order transition. Besides the transition from the BCS phase to the EHP we would also expect a transition similar to the Mott transition in a repulsive Hubbard model. This is due to the fact that there is always competition between kinetic energy and interaction energy. In the strongly interacting regime the interaction suppresses the kinetic energy and an insulating Mott phase appears [47,48]. A similar effect is expected for our electron–hole system in the strongly interacting regime.

Before we provide a more detailed mean-field calculation, let us give a brief qualitative discussion of the electron–hole system. The properties of the system are controlled by three parameters, namely the Fermi energy, the interaction strength and the temperature. The influence of these parameters one can understand in terms of the free energy in Eq. (8) as follows: (i) changing the Fermi energy E_F results in a change of the density; (ii) an increase of the temperature implies an increase of the thermal fluctuations of the electron–hole gas; (iii) finally, increasing the interaction (e.g., by reducing the distance D between the layers or replacing the dielectric with a different dielectric constant ε), will reduce the size of the Cooper pairs in the BCS regime. The last means that with the screened Coulomb interaction in (3) an increasing interaction means a decreasing size of Cooper pairs, namely the appearance of Cooper pairs with larger values of q. This is easy to justify by using the linearized mean-field equation $\delta F/\delta \Delta_{\mathbf{q}} = 0$ for small $\Delta_{\mathbf{q}}$ that gives

$$\Delta_{\mathbf{q}} \sim f_1 \frac{\hbar \bar{U} e^{-qD/\hbar}}{q + a} \Delta_{\mathbf{q}} \tag{9}$$

with a positive prefactor f_1, which is independent of $\bar{U}$. This equation has a nonzero solution (i.e., a Cooper pair) if the factor in front of $\Delta_{\mathbf{q}}$ on the right-hand side is 1. For large values of $\bar{U}$ this is the case only for a sufficiently large value of q. Below we focus on the mean-field theory alone, using Eq. (8) for the free energy and study the crossover to strong interaction and high densities within this approach.

4. Phase diagram of a translational invariant system

The free energy expression (8) is now considered for a translational invariant system with weak interaction. In this case we expect that the order parameter is uniform, i.e. is independent on the momentum: $\Delta_{\mathbf{q}} = \Delta$. This means that the Cooper pairs are extended object, which may be justified at least for weak interaction $u_0 << E_F$, where u_0 is defined as the Fourier component of the inverse Coulomb interaction $1/u_0 = \int_{q \le q_F} (1/U_{\mathbf{q}}) d^2q/(2\pi q_F)^2$. Then the free energy in Eq. (8) reduces, up to the dimensionless order parameter $\gamma = \beta|\Delta|$ independent term, to

$$F = -\frac{(k_B T)^2}{u_0}\left[\gamma^2 + \frac{u_0}{E_F}\frac{1}{4\pi}\int_{-E_F/k_B T}^{(E_b - E_F)/k_B T} \ln\left(1 + \frac{\cosh(\sqrt{Ry^2 + \gamma^2}) - 1}{2\cosh^2(y/2)}\right) dy\right]. \tag{10}$$

The integrand in Eq. (10) is a symmetric function of $y \equiv (E_q - E_F)/(k_B T)$ which implies that the integral is a symmetric function of E_F with respect to $E_F = E_b/2$. This property reflects the particle–hole symmetry of the underlying fermionic Hamiltonian.

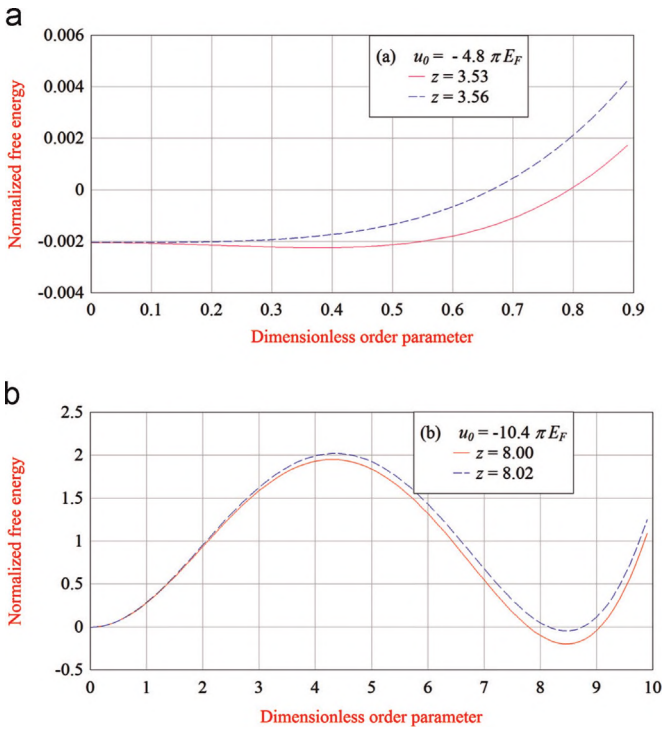

Fig. 3. The free energy, normalized by $-(k_B T)^2/u_0$, as a function of the dimensionless order parameter γ for different parameter $z = E_F/k_B T$ for the upper band edge $E_b = 7k_B T$ and $R = 10^{-3}$. The curves are shifted with respect to each other to show the relative behavior of the normalized free energy as a function of the dimensionless order parameter. (a) The second order phase transition for weak interaction ($u_0 = -4.8\pi E_F$) at z=3.54. (b) The first order phase transition for a strong interaction ($u_0 = -10.4\pi E_F$) at z=8.01.

Below the results of the calculations for the free energy of the electron–hole pairs in GaAs/AlGaAs quantum wells are presented. For these CQWs the interaction strength is $\bar{U} = 1.558 \times 10^5$ eV/m. For example, for InGaAs and ZnCdSe/ZnSe quantum wells the interaction strength is given by $\bar{U} = 4.009 \times 10^5$ eV/m and $\bar{U} = 2.426 \times 10^5$ eV/m, respectively. As an example we have plotted in Fig. 3 the free energy as a function of γ for different parameter $z = E_F/k_B T$ and specific values of E_F/u_0 and E_b. The analysis of the results presented in Fig. 3 shows that there is apparently a second order transition at $u_0 = 4.8\pi E_F$ and a first order transition for a stronger Coulomb interaction $u_0 = 10.4\pi E_F$ from the BCS phase at $E_F < E_c$ to a state with vanishing order parameter.

At lower densities there is a conventional BCS transition from a low-density EHP to a superfluid phase. In order to describe the phase transition scenario in more detail, we consider the case where the order parameter is small, which is a realistic situation. Thus, we can expand the free energy and present it in the Landau form as

$$F(\Delta) = F_0 + F_2\gamma^2 + F_4\gamma^4 + F_6\gamma^6 + O(\gamma^8), \tag{11}$$

where we call the polynomial up to γ^6 the truncated free energy $\mathcal{F}_6(\gamma)$. The latter allows us to discuss the phase diagram of the electron–hole system in a simple manner. First of all, the stability of the system requires $F_6 > 0$. Then there are two different phases due to minima of truncated free energy, namely one for $\gamma > 0$ (superfluid phase) and another one for $\gamma = 0$ (electron–hole plasma). There are two different types of a transition between these phases: a first order and a second order transition. They are distinguished by the fact that the position of the minima γ_0 goes continuously (second order transition) or discontinuously (first

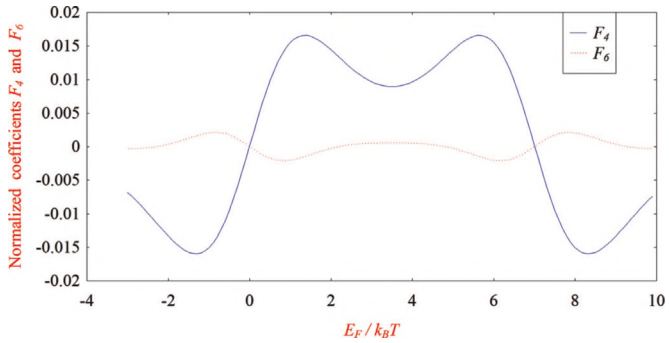

Fig. 4. The Landau coefficients F_4 and F_6 of the free energy of Eq. (11), normalized by $-(k_B T)^2/u_0$, as functions of $E_F/k_B T$ for $E_b = 7k_B T$. They are symmetric with respect to the band center $E_F = E_b/2$.

order transition) to zero. In terms of our truncated free energy $\mathcal{F}_6(\gamma)$, the second order transition is characterized by one minimum at $\gamma = 0$, which is realized for $F_2 > 0$, and by a maximum at $\gamma = 0$ and another minimum at $\gamma > 0$. The latter is realized for $F_4 > 0$ and $F_2 < 0$. The first order transition, on the other hand, is characterized by two minima and a maximum in between. This is realized for $F_4 < 0$, F_2, $F_6 > 0$. The transition point is given by the degeneracy of the two minima of $\mathcal{F}_6(\gamma)$, namely for $\mathcal{F}_6(\gamma_+) = \mathcal{F}_6(0) = F_0$ with

$$\gamma_+^2 = -\frac{F_4}{3F_6} + \sqrt{\frac{F_4^2}{9F_6^2} - \frac{F_2}{3F_6}}. \tag{12}$$

The coefficients F_4 and F_6 are plotted as functions of the Fermi energy in Fig. 4, showing the particle–hole symmetry with respect to the band center $E_F = E_b/2$.

A closer inspection of condition $\mathcal{F}_6(\gamma_+) = \mathcal{F}_6(0)$ leads to the condition (cf. Appendix A)

$$F_4^2 = 4F_2F_6 \tag{13}$$

for the phase transition. This equation and the condition for a second order phase transition $F_2 = 0$, $F_4 > 0$ shall be used in the subsequent section to evaluate the phase diagram of the electron–hole gas.

The phase diagram of the electron–hole system within mean-field approximation is depicted in Fig. 5, which clearly shows a paired BCS phase under the dome and a non-BCS phase above the dome. This structure indicates that for a sufficiently strong interaction at intermediate densities the electron–hole system has a tendency to form paired states. At lower or at higher densities there is no pairing effect. The horizontal line at $E_F/u_0 \approx 0.04$ is important. It separates the strongly interacting regime from the

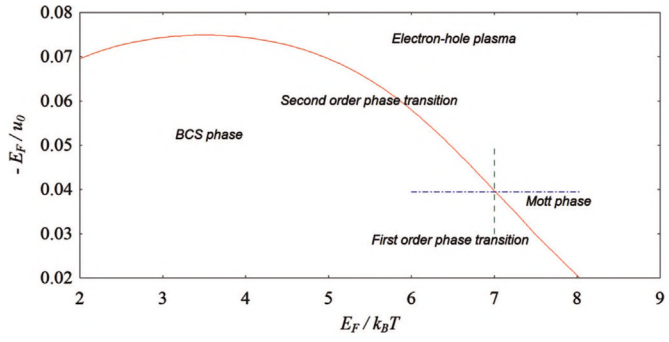

Fig. 5. Phase diagram of the electron–hole system with attractive interaction. The phase boundary continuous symmetrically to lower values of the Fermi energy (not plotted here). The horizontal dashed line separates the weak from the strong interaction regime, the vertical line is the upper band edge $E_b = 7k_B T$.

weakly interacting regime, which can be distinguished by the fact that the former has a first order transition to the non-BCS phase and the latter has a second order transition (see also Fig. 3). If the pairing order parameter vanishes, the electron–hole system is just a gas of unpaired electrons and holes with the Hamiltonian in the mean-field approximation: $H_0 = \sum_{\mathbf{k}} \sum_{\sigma=e,h} (\epsilon_{\mathbf{k},\sigma} - \mu_\sigma) c^\dagger_{\mathbf{k}\sigma} c_{\mathbf{k}\sigma}$. The interaction is taken care of by a renormalized chemical potential μ_σ. If the Fermi energy $E_F = \mu_e + \mu_h$ is inside the band (i.e., for $0 < E_F$, $E_F < E_b$) this describes an electron–hole plasma. On the other hand, if the Fermi energy is above the band (i.e, for $E_F > E_b$) there are no extended (Bloch) states and the system is in a localized phase.

5. Discussion

As a result of our mean-field approach we have found that the electron–hole system in two separate layers has three different characteristic regimes. According to the phase diagram in Fig. 5, there is a dilute electron–hole gas at weak interaction without pairing of electrons and holes in the two layers. In other words, the interaction is too weak to create pairing, therefore, the electrons and the holes are independent. The effect of the interaction in this phase is a renormalization of the Fermi energy, as it can be analyzed by a Hartree–Fock approximation. The corresponding fermionic quasi-particle spectrum has two branches, namely

$$E_{q,e} = \frac{q^2 - q_F^2}{2m_e}, \quad E_{q,h} = \frac{q^2 - q_F^2}{2m_h}. \tag{14}$$

Either by increasing the densities or by increasing the interaction strength a second order phase transition to a BCS phase with Cooper pairs appears. The corresponding fermionic quasi-particle excitation spectrum with the characteristic BCS gap is obtained from Eqs. (1) and (7) in the form of the Bogoliubov–De Gennes Hamiltonian [2], whose spectrum has also two branches:

$$E_{q,\Delta} = \frac{q^2 - q_F^2}{4m_+} \pm \sqrt{\left(\frac{q^2 - q_F^2}{4m_-}\right)^2 + \Delta^2}. \tag{15}$$

Being in the BCS phase we can either increase the Fermi energy or increase the electron–hole interaction. In the latter the Cooper pairs become increasingly tighter but the physics will not change by a phase transition. This is also what we see in the phase diagram of Fig. 5. However, if we increase the Fermi energy we will eventually cross the phase boundary and leave the BCS phase. There are two possible reasons for this transition: one is simply pair breaking by particle-particle collisions, the other one is that the Fermi energy is above the band if $E_F > E_b$. In the latter case Cooper pairing is not possible any more, even at arbitrarily low temperatures. Moreover, there is also thermal pair breaking which appears on the left-hand side of our phase diagram.

As already discussed in the Introduction, we can compare the quasiparticle spectrum of the BCS phase with that of the Mott phase, which appears for $q_F > q_b$. In the latter we also find two bands, separated by a gap

$$\Delta_M = (q_F^2 - q_b^2)\left(\frac{1}{2m_e} + \frac{1}{2m_h}\right). \tag{16}$$

The lower band is for the electron, the upper band is for holes now. If the electron band is completely filled, excitations have to overcome the gap Δ_M or they stay in the Fermi sea. On the other hand, individual electrons cannot be excited if the Coulomb attraction is much larger than Δ_M. Then only coupled electron–hole pairs can be excited. This leads to an effective systems of hard-core bosons. Its excitations also have to overcome the gap Δ_M. This phase can be

understood as a bosonic Mott phase. Since the Mott phase is commensurate with the underlying lattice, the phase transition from the BCS phase must be of the first order.

The BCS phase is an insulator, since the electron–hole Cooper pair is charge-neutral and cannot be driven by electric field, while the EHP is the conducting state, because the electrons and holes in the presence of the electric field can move in opposite directions, conducting current. Moreover, at high densities and strong attractive interaction the electron–hole pairs form composite bosons. Phase coherence, the hallmark of the BCS state, would be destroyed by intensive collisions of the particles. The ground state is a bosonic Mott phase, the counterpart of the fermionic Mott phase [48]. This is a kind of charge density wave, where its wavevector agrees with the states at the band edge. The transition to the Mott phase can be observed at small interlayer separation D and high electron and hole densities. We study the phase diagram of the electron–hole system formed in two layers within a mean-field approximation for the pairing order parameter as a function of interaction strength, temperature and density. The calculation includes a Landau expansion in terms of the pairing order parameter. For realistic systems of CQWs and two GLs we consider the case where the masses of the electrons and holes are different. This difference results in the extra term in the BCS equation for the free energy. Besides, we analyze the order of the phase transitions with respect to the temperature as well as the temperature dependence of the order parameter, using the results of the mean-field calculations at nonzero temperatures.

The phase transition from the BCS phase to the EHP could be observed, for example, in the following transport experiment: if an external electric field is applied, the BCS phase cannot be driven by the electric field, since electron–hole Cooper pair is charge neutral, while in the EHP the electrons and holes move in opposite directions, conducting current. The wave vector of the EHP is given by the maximal wave vector q_F of the electron–hole spectrum. The bosons of the Mott phase are also charge neutral. Therefore, they can only be distinguished from the EHP but not from BCS phase. The BCS-Mott transition, however, should be observable from the statistics of the quasiparticles, which is fermionic in the BCS phase but bosonic in the Mott phase.

In the former case the paired gas undergoes another second order phase transition to a dense electron–hole gas, whereas in the latter case it is possible that we have a first order transition from the BCS phase to the EHP. The wave vector of the EHP is given by the maximal wave vector of the electron–hole spectrum $\epsilon_{\mathbf{k},e} + \epsilon_{\mathbf{k},h}$. The phase diagram in a two-layer electron–hole system can also be characterized with the help of the Landau expansion in Eq. (11) by (a) weak interaction at low/high density: $F_2, F_4 > 0$, $\gamma = 0$ (EHP), (b) weak interaction at intermediate density: $F_2 < 0$, $F_4 > 0$, $\gamma > 0$ (BCS), (c) strong interaction at low/high density: $F_2 > 0$, $F_4 < 0$, $F_6 > 0$, $\gamma = 0$ for $E_F > E_b$ (MI), and (d) strong interaction at intermediate density: $F_2 > 0$, $F_4 < 0$, $F_6 > 0$, $\gamma > 0$ (BCS).

The estimation of the physical parameters, using the results from experimental measurements on coupled quantum wells, indicates that the values $u_0 \approx 10^{-4}$ eV, $E_F \approx 10^{-3}$ eV and $k_B T \approx 10^{-4}$ eV are in or close to the regime of strong interaction and high density. The remaining problem is the bandwidth E_b, which is for typical semiconductors 1 eV. Therefore, the Mott transition is not accessible in conventional semiconductors due to the bandwidth being much larger than the typical Coulomb interaction u_0 and Fermi energy E_F. However, it might be possible to create special narrow band materials and correspondingly large Fermi energies by appropriate doping. A possible candidate is a graphene double layer, where the chemical potential of the electrons and hole can be tuned separately by external gates. Another advantage of this material is that the mass of the electrons and the holes can be tuned by a spectral gap in the electronic spectrum [41]. The latter is created by breaking the sublattice symmetry of the honeycomb lattice. The discovery of new 2D materials might open more opportunities. Finding the proper material seems to be the main challenge for the experimental observation of the Mott transition.

6. Conclusions

The BCS-like mean-field approach has provided the phase diagram with several phases and phase transitions for the electron–hole system in two layers with spatially separated electrons and holes. For weak interaction and low densities we have found a second order transition from electron–hole plasma to a conventional BCS phase with electron–hole Cooper pairs. With increasing density there is another transition from the BCS phase to a bosonic Mott phase at strong electron–hole interaction. The latter can be obtained by reducing the interlayer separation D and/or replacing the dielectric with different dielectric constant ε. At the first order transition from the BCS phase to the Mott phase, the Fermi energy coincides with the upper band edge of the electron–hole spectrum. The observation of this first order transition requires a Fermi energy being above the upper band edge of the electron–hole spectrum. A possible approach could be based on strong doping of narrow-band semiconductors.

Acknowledgments

The authors acknowledge support from the Center for Theoretical Physics of the New York City College of Technology, CUNY. R.Ya.K. acknowledges the support of the US Army Research Office, Grant #64775-PH-REP. O.L.B. acknowledges the support of KITP, Santa Barbara under National Science Foundation Grant no. PHY1125915 and their kind hospitality at the early stages of this project.

Appendix A. First order phase transition

The first order phase transition is characterized by $\mathcal{F}_6(\gamma_+) = \mathcal{F}_6(0)$ which also reads

$$F_2\gamma_+^2 + F_4\gamma_+^4 + F_6\gamma_+^6 = 0. \tag{17}$$

For $\gamma_+ > 0$ we have two solutions of this quadratic condition as

$$\gamma_+^2 = -\frac{F_4}{2F_6} \pm \sqrt{\frac{F_4^2}{4F_6^2} - \frac{F_2}{F_6}}. \tag{18}$$

This must be compared with the definition of γ_+^2 in Eq. (12), which yields for $\zeta = F_2F_6/F_4^2$ the equations

$$1 \pm m3\sqrt{1-4\zeta} - 2\sqrt{1-3\zeta} = 0. \tag{19}$$

Both Eqs. (12) and (19) are solved with $\zeta = 1/4$ such that

$$F_4^2 = 4F_2F_6. \tag{20}$$

References

[1] J.R. Schrieffer, Theory of Superconductivity, Benjamin, New York, 1964.
[2] P.G. De Gennes, Superconductivity of Metals and Alloys, W. A. Benjamin, New York, 1966.
[3] M.P.A. Fisher, P.B. Weichman, G. Grinstein, D.S. Fisher, Phys. Rev. B 40 (1989) 546.
[4] S. Sachdev, Quantum Phase Transitions, Second ed., Cambridge University

Press, Cambridge, 1990.
[5] W.F. Brinkman, T.M. Rice, Phys. Rev. B 7 (1973) 1508.
[6] R.A. Höpfel, J. Shah, A.C. Gossard, Phys. Rev. Lett. 56 (1986) 765.
[7] M. Greiner, O. Mandel, T. Esslinger, T.W. Hänsch, I. Bloch, Nature 415 (2002) 39.
[8] Yu.E. Lozovik, V.I. Yudson, Sov. Phys. JETP Lett. 22 (1975) 26;
Yu.E. Lozovik, V.I. Yudson, Sov. Phys. JETP 44 (1976) 389.
[9] S.I. Shevchenko, Phys. Rev. Lett. 72 (1994) 3242.
[10] I.V. Lerner, Yu.E. Lozovik, Sov. Phys. JETP 47 (1978) 146;
I.V. Lerner, Yu.E. Lozovik, Sov. Phys. JETP 49 (1979) 376.
[11] A.B. Dzjubenko, Yu.E. Lozovik, J. Phys. A 24 (1991) 415.
[12] C. Kallin, B.I. Halperin, Phys. Rev. B 30 (1984) 5655;
C. Kallin, B.I. Halperin, Phys. Rev. B 31 (1985) 3635.
[13] D.S. Chemla, J.B. Stark, W.H. Knox, in: J.-L. Martin (Ed.), Ultrafast Phenomena VIII, vol. 21, Springer, Berlin, 1993;
C.W. Lai, J. Zoch, A.C. Gossard, D.S. Chemla, Science 303 (2004) 503.
[14] D. Yoshioka, A.H. MacDonald, J. Phys. Soc. Jpn. 59 (1990) 4211.
[15] Xu. Zhu, P.B. Littlewood, M.S. Hybertsen, T.M. Rice, Phys. Rev. Lett. 74 (1995) 1633.
[16] S. Conti, G. Vignale, A.H. MacDonald, Phys. Rev. B 57 (1998) R6846.
[17] M.A. Olivares-Robles, S.E. Ulloa, Phys. Rev. B 64 (2001) 115302.
[18] D. Snoke, S. Denev, Y. Liu, L. Pfeiffer, K. West, Nature 418 (2002) 754.
[19] D. Snoke, Science 298 (2002) 1368.
[20] L.V. Butov, A. Zrenner, G. Abstreiter, G. Bohm, G. Weimann, Phys. Rev. Lett. 73 (1994) 304;
L.V. Butov, C.W. Lai, A.L. Ivanov, A.C. Gossard, D.S. Chemla, Nature 417 (2002) 47;
L.V. Butov, A.C. Gossard, D.S. Chemla, Nature 418 (2002) 751.
[21] V.V. Krivolapchuk, E.S. Moskalenko, A.L. Zhmodikov, Phys. Rev. B 64 (2001) 045313.
[22] A.V. Larionov, V.B. Timofeev, J. Hvam, K. Soerensen, Sov. Phys. JETP 90 (2000) 1093;
A.V. Larionov, V.B. Timofeev, Sov. Phys. JETP Lett. 73 (2001) 301.
[23] T. Fukuzawa, E.E. Mendez, J.M. Hong, Phys. Rev. Lett. 64 (1990) 3066;
J.A. Kash, M. Zachau, E.E. Mendez, J.M. Hong, T. Fukuzawa, Phys. Rev. Lett. 66 (1991) 2247.
[24] U. Sivan, P.M. Solomon, H. Shtrikman, Phys. Rev. Lett. 68 (1992) 1196.
[25] S.A. Moskalenko, D.W. Snoke, Bose–Einstein Condensation of Excitons and Biexcitons and Coherent Nonlinear Optics with Excitons, Cambridge University Press, New York, 2000.
[26] J.P. Eisenstein, A.H. MacDonald, Nature (London) 432 (2004) 691.
[27] O.L. Berman, Yu.E. Lozovik, D.W. Snoke, R.D. Coalson, Phys. Rev. B 70 (2004) 235310.
[28] Y.N. Joglekar, A.V. Balatsky, S. Das Sarma, Phys. Rev. B 74 (2006) 233302.
[29] D.W. Snoke, Quantum gases: finite temperature and non-equilibrium dynamics, in: N.P. Proukakis, S.A. Gardiner, M.J. Davis, M.H. Szymanska (Eds.), Cold Atoms Series, vol. 1, Imperial College Press, London, 2013.
[30] K. Das Gupta, A.F. Croxall, J. Waldie, C.A. Nicoll, H.E. Beere, I. Farrer, D.A. Ritchie, M. Pepper, Adv. Condens. Matter Phys. 2011 (2011) 727958.
[31] L.V. Butov, J. Phys.: Condens. Matter 19 (2007) 295202.
[32] M. Stern, V. Garmider, V. Umansky, I. Bar-Joseph, Phys. Rev. Lett. 100 (2008) 256402.
[33] D.W. Snoke, J.D. Crawford, Phys. Rev. E 52 (1995) 5796.
[34] D.W. Snoke, Solid State Commun. 146 (2008) 73.
[35] D. Semkat, F. Richter, D. Kremp, G. Manzke, W.-D. Kraeft, K. Henneberger, Phys. Rev. B 80 (2009) 155201.
[36] G. Manzke, D. Semkat, H. Stolz, New J. Phys. 14 (2012) 095002.
[37] I. Sodemann, D.A. Pesin, A.H. MacDonald, Phys. Rev. B 85 (2012) 195136.
[38] Yu.E. Lozovik, S.L. Ogarkov, A.A. Sokolik, Phys. Rev. B 86 (2012) 045429.
[39] R.E.V. Profumo, M. Polini, R. Asgari, R. Fazio, A.H. MacDonald, Phys. Rev. B 82 (2010) 085443.
[40] A. Perali, D. Neilson, A.R. Hamilton, Phys. Rev. Lett. 110 (2013) 146803.
[41] O.L. Berman, R.Ya. Kezerashvili, K. Ziegler, Phys. Rev. B 85 (2012) 035418.
[42] M.E. Portnoi, I. Galbraith, Phys. Rev. B 60 (1999) 5570.
[43] M. Steger, C. Gautham, B. Nelsen, D. Snoke, L. Pfeiffer, K. West, Appl. Phys. Lett. 101 (2012) 131104.
[44] D. Snoke, Nat. Nanotechnol. 8 (2013) 393.
[45] D. Ballarini, et al., Nat. Commun. 4 (2013) 1778.
[46] K. Ziegler, Laser Phys. 15 (2005) 650.
[47] N.F. Mott, Rev. Mod. Phys. 40 (1968) 677.
[48] N.F. Mott, Metal Insulator Transitions, Taylor & Francis, London, 1990.